

# No Fossil Disk in the T Tauri Multiple System V 773 Tau

G. Duchêne, A. M. Ghez, C. McCabe

*Division of Astronomy and Astrophysics, UCLA, Los Angeles, CA 90095-1562*

duchene@astro.ucla.edu

A. J. Weinberger

*Department of Terrestrial Magnetism, Carnegie Institution of Washington, Washington, DC 20015*

## ABSTRACT

We present new multi-epoch near-infrared (NIR) and optical high-angular images of the V 773 Tau pre-main sequence triple system, a weak-line T Tauri (WTTS) system in which the presence of an evolved, “fossil” protoplanetary disk has been inferred on the basis of a significant infrared (IR) excess. Our images reveal a fourth object bound to the system, V 773 Tau D. While it is much fainter than all other components at  $2\,\mu\text{m}$ , it is the brightest source in the system at  $4.7\,\mu\text{m}$ . We also present medium-resolution  $K$  band adaptive optics spectroscopy of this object, which is featureless with the exception of a weak  $\text{Br}\gamma$  emission line. Based on this spectrum and on the spectral energy distribution (SED) of the system, we show that V 773 Tau D is another member of the small class of “infrared companions” (IRCs) to T Tauri stars (TTS). It is the least luminous, and probably the least massive, component of the system, as opposed to most other IRCs, which suggests that numerous low-luminosity IRCs such as V 773 Tau D may still remain to be discovered. Furthermore, it is the source of the strong IR excess in the system. We therefore reject the interpretation of this excess as the signature of a fossil (or “passive”) disk and further suggest that these systems may be much less frequent than previously thought.

We further show that V 773 Tau C is a variable classical TTS (CTTS) and that its motion provides a well constrained orbital model. We show that V 773 Tau D can be dynamically stable within this quadruple system if its orbit is highly inclined. Finally, V 773 Tau is the first multiple system to display such a variety of evolutionary states (WTTS, CTTS, IRC), which may be the consequence of the strong star-star interactions in this compact quadruple system.

*Subject headings:* stars: individual (V 773 Tau) — binaries: close — stars: pre-main sequence — planetary systems: protoplanetary disks

## 1. Introduction

V 773 Tau (HD 283447, HBC 367) is a remarkable  $\sim 5$  Myr-old,  $\sim 1.5 M_{\odot}$  (White & Ghez 2001) pre-main sequence object located 148 pc away (Lestrade et al. 1999) in the Taurus star-forming region. Its SED displays two broad maxima at  $\sim 1 \mu\text{m}$  and  $\sim 20 \mu\text{m}$  (cf, e.g., data compilation by Feigelson et al. 1994). The first one corresponds roughly to what is expected for a stellar photosphere, while the longer wavelength component is reminiscent of the spectral energy distribution (SED) of accreting pre-main sequence stars, i.e. classical T Tauri stars (CTTS). This infrared (IR) excess in CTTS is generally attributed to a dusty circumstellar disk heated by reprocessing of starlight and by energy released through the accretion process. While the IR excess in V 773 Tau suggests a disk model for this system, the weak hydrogen emission lines in its spectrum (e.g., Cabrit et al. 1990) implies that no accretion is ongoing on the stars, consistent with a weak-line T Tauri star (WTTS), although the presence of forbidden emission lines in its spectrum imply mass loss. This has been considered as substantial evidence for the presence of a “passive disk” around the stars, i.e., a non-accreting dusty structure that only reprocesses the stellar light. Furthermore, Phillips et al. (1996) first pointed out that, because of the dip around  $2 \mu\text{m}$  in the SED of V 773 Tau, this object presents the characteristics of a “fossil disk”, as defined by Strom (1995), in which the inner parts of the disk have been cleared out of small dust grains possibly through the formation of planetesimals. In other words, this system has been proposed to be one of the few “transition objects” between CTTS and WTTS, observed during the phase of disk dissipation. This duality WTTS/IR excess is present in only a few objects (e.g., Skrutskie et al. 1990; Stassun et al. 2001), which suggests that this is a short-lived phase.

While the analysis of the SED and the emission lines have been based on low angular resolution data sets, high angular and spectral resolution studies have resolved this object into a triple system. First, a tight ( $\sim 0''.1 \approx 15$  AU) stellar companion was discovered through speckle imaging (Ghez, Neugebauer & Matthews 1993; Leinert et al. 1993). The primary component of this pair later appeared to be itself double, a 51 day-period ( $\sim 0.3$  AU semi-major axis; Welty 1995) double-lined spectroscopic binary (SB). All three components are believed to be WTTS (White & Ghez 2001). Interactions between the various components are likely to be important in this tight multiple star system. Indeed, the variable non-thermal radio emission observed in this system (O’Neal et al. 1990; Dutrey et al. 1996) appears to be phase-locked with the SB (Massi, Menten & Neidhöfer 2002). This emission therefore appears to be chromospheric with enhanced activity occurring when the two stellar chromospheres partially overlap at periastron. The properties of the putative fossil disk could also be affected by the multiplicity of this object. A fit of a disk emission model to the IR excess places the inner radius of the optically thick disk at about  $\sim 0.2$  AU. This is well inside the orbit of the SB, raising doubts about the disk model.

In this paper, we present new near-infrared (NIR) and optical high-angular resolution imaging of V 773 Tau, which unambiguously reveal a fourth component. The observed 1.6–4.7  $\mu\text{m}$  colors and the broadband 2  $\mu\text{m}$  spectrum of this object show that it is an infrared companion (IRC) and that it is in fact the source of the IR excess in this system. Throughout this paper, we will refer to the SB as V 773 Tau AB, the long-known speckle companion as V 773 Tau C and the new companion identified in this study as V 773 Tau D. We present the various datasets used in this paper in § 2. The orbital motion of V 773 Tau C and the photometric properties of all components of the system are analyzed in § 3. In § 4, we determine the status of each component and study the importance of star-star interactions in the system. Finally, we summarize our results in § 5.

## 2. Observations and data analysis

### 2.1. Speckle imaging

V 773 Tau has been regularly targeted by speckle interferometry surveys because, as a  $\sim 0''.1$  binary, it is an excellent candidate for studies of orbital motion. A number of measurements (see Table 1) have already been reported (Leinert et al. 1993; Ghez et al. 1993, 1995, 1997; Woitas, Köhler & Leinert 2001, Tamazian et al. 2002).

We present here several new NIR speckle observations of the system. These data were obtained at 2.2  $\mu\text{m}$  ( $K$  band) on 1996 Oct 24, 1997 Nov 19, 1998 Nov 04, 1999 Nov 20 and 2000 Dec 08 at the 200-inch telescope at Palomar Observatory and on 2001 Dec 08 at the 10m Keck I telescope. We used a 64x64 subsection of a 256x256 SRBC InSb array at Palomar and the facility instrument Near-IR Camera (Matthews & Soifer 1994; Matthews et al. 1996) at Keck. These instruments offer pixel scales of  $0''.0337 \pm 0''.0005/\text{pixel}$  and  $0''.0203 \pm 0''.0003/\text{pixel}$  respectively, adequately sampling the diffraction limit in the  $K$  band ( $\sim 0''.09$  and  $\sim 0''.05$ ), and have known orientations to an accuracy of  $\pm 1^\circ$ . Stacks of several hundred short integration ( $t \sim 0.1\text{s}$ ) exposures were obtained, immediately followed by a similar stack of exposures on a calibration point source. Standard speckle data reduction routines were applied to the data; we refer the reader to Ghez et al. (1993) and Patience et al. (1998) for more details. Examples of power spectra at various epochs are presented in Figure 1.

In the latter four epochs, the calibrated power spectra of the system reveal two distinct sets of fringes, corresponding to the V 773 Tau AB–C and V 773 Tau ABC–D pairs<sup>1</sup>. In those

---

<sup>1</sup>The second set is in fact the sum of the V 773 Tau AB–D and V 773 Tau C–D almost parallel sets of

cases, we first fit the better-defined V 773 Tau AB–C pair, then divide the observed power spectrum of the system by a model of this binary and finally fit a second binary system. The information regarding the V 773 Tau AB–D pair is then easily recovered via the known separation and flux ratio of V 773 Tau AB–C. A regular binary system model is fit to the other datasets, which do not show sufficient evidence for a third resolved component<sup>2</sup>.

We also present here the results of a visible wavelength speckle interferometry experiment performed on 1991 Sep 25 to 29 at the 200-inch telescope at Palomar Observatory with the same setup as that described by Gorham et al. (1992). The filters used,  $F_{620}$ ,  $F_{656}$ ,  $F_{800}$  and  $F_{850}$ , are all 100 Å wide and are centered on 6200, 6560, 8000 and 8500 Å respectively. Data reduction and analysis routines are also similar to that described by Gorham et al. (1992), in which autocorrelation functions (ACFs) are generated. While ACFs are related to the power spectrum analyzed for the IR data, they are more robustly generated in photon-counting experiments. Only two stars are identified in our data, which are readily associated with V 773 Tau AB and C.

## 2.2. Adaptive optics imaging

### 2.2.1. $H$ & $K$ band imaging

In addition to this wealth of speckle measurements, we also obtained  $H$  band<sup>3</sup> and  $K$  band adaptive optics (AO) images of the V 773 Tau system with the AO system of the 10 m Keck II telescope (Wizinowich et al. 2000) and the facility NIR spectrometer NIRSPEC (McLean et al. 2000). The data were obtained on 2000 Nov 20 with SCAM, the slit-viewing camera inside NIRSPEC. With each filter, we obtained 4 sets of 100 individual 0.1 s exposures, with the object centered on a different part of the detector in each set. The

---

fringes, which we treat as a single fringe pattern corresponding to V 773 Tau D and the photocenter of V 773 Tau ABC.

<sup>2</sup>In the 1997 dataset, the V 773 Tau AB–C is not clearly resolved although the amplitude of the power spectrum decreases towards the outer edge of the power spectrum along  $PA \sim 40^\circ$  (see Figure 1). Since we do not detect the first minimum of the visibility curve along this direction, we can only set an upper limit on the binary separation ( $\lesssim \lambda/2D \approx 45$  mas in the  $K$  band with the Palomar 200-inch telescope). In subsequent epochs, this first minimum is reached and the binary parameters can be confidently derived.

<sup>3</sup>The filter we used, “NIRSPEC-3”, is a customized filter specific to the instrument. Its central wavelength ( $\lambda_c = 1.625 \mu\text{m}$ ) and bandwidth ( $\Delta\lambda = 0.36 \mu\text{m}$ ) are close enough to the standard broadband  $H$  filter ( $\lambda_c = 1.630 \mu\text{m}$ ,  $\Delta\lambda = 0.31 \mu\text{m}$ ) that we do not expect magnitude differences larger than a few hundredths. Throughout our paper, we therefore refer to this filter as the  $H$  filter.

individual exposure time was short enough to avoid saturating the stellar cores. V 773 Tau is bright enough in the visible ( $V \sim 10.7$ ,  $R \sim 9.8$ ) and is unresolved in the wavefront sensor camera so it could be used as a natural guide star for the AO system. We achieved Strehl ratios of 12 % and 15 % respectively at  $H$  and  $K$ , which is enough to provide diffraction-limited cores. The resolution of the images, measured as the FWHM of a Gaussian fit to the radial profile of the brightest component, V 773 Tau AB, are about 40 and 50 mas at  $H$  and  $K$ , respectively. The final images are presented in Figure 2 (upper row).

Data reduction included sky subtraction, flat-fielding, bad pixel removal and shift-and-add the individual images and was performed in IRAF<sup>4</sup>. Astrometry and relative photometry are performed through two methods. First, we estimate the centroid locations for each component in the final image. To estimate uncertainties, we perform the same analysis on four subsets of the data and calculate their standard deviation. Relative photometry is obtained by summing fluxes over 2-pixel radius apertures around each component; uncertainties are similarly obtained through subsets of the data. To avoid potential star-to-star flux contamination, we also fit point spread functions (PSFs) to the multiple system. Because of the limited field of view of SCAM, no other star is available to be used as a contemporaneous PSF. We thus use both a theoretical image which is basically the Fourier transform of the entrance pupil of the telescope and an empirical PSF with a somewhat better image quality, which we obtained on Nov 19 by imaging T Tau N (see Duchêne, Ghez & McCabe 2002 for details). All three techniques agree within  $3\sigma$  of each other and all trends are naturally explained by the different imperfections in the PSFs. The final astrometric and photometric results presented in Table 1 are the averages of these three techniques (one direct measurement and two fits).

### 2.2.2. $L'$ & $M'$ band imaging

We also imaged vt at  $3.8\mu\text{m}$  and  $4.7\mu\text{m}$  ( $L'$  and  $M'$  broadband filters, which are  $0.7\mu\text{m}$  and  $0.24\mu\text{m}$  wide respectively) with the new facility instrument NIRC2 (Matthews et al., in prep.) behind the AO system on the Keck II telescope. The data were obtained on 2002 December 13 under excellent seeing conditions; V 773 Tau itself was used as a natural AO guide star. Strehl ratios on order of 60-75 % were measured at  $L'$  on similarly bright single stars throughout the night. A circular cold mask equivalent to a circular 9 m-diameter entrance pupil was used to minimize the background emission, a critical factor in the thermal

---

<sup>4</sup>IRAF is distributed by the National Optical Astronomy Observatories, which is operated by the Association of Universities for Research in Astronomy, Inc., under contract to the National Science Foundation.

IR range. The resulting diffraction-limited images have Gaussian FWHM of 90 and 110 mas at  $L'$  and  $M'$ , respectively.

Several hundred short exposures ( $\sim 0.05$  s each) were obtained at four different locations on the detector for a total integration time of about 1 min with each filter. The datasets were subtracted from each other to remove the thermal background, flat-fielded, corrected for bad pixels and shift-and-added to produce the final images presented in Figure 2 (lower row). Astrometric and photometric parameters of the multiple systems were obtained using the same methods as described above for the  $H$  and  $K$  images. The PSF fitting process is performed using HD 1160 (a single star) at  $L'$  and T Tau N at  $L'$  and  $M'$ . Both were observed on the same night with the same setup. All methods yield compatible estimates within  $\sim 2\sigma$  for both the location of the centroids and the flux ratios.

### 2.3. Adaptive optics spectroscopy

On 2000 Nov 20, we also obtained long-slit  $K$  band spectroscopy of two components of the system, by aligning the  $0''.036$ -wide slit of NIRSPEC along the V 773 Tau AB–V 773 Tau D position angle. Four spectra were obtained at different locations behind the slit, with a total integration time of 10 minutes. The instrumental setup is identical to that used in our previous study of the tight binary T Tau S reported in Duchêne et al. (2002), which also provides more details on the data reduction process. The spectra cover the  $2.0$ – $2.4\,\mu\text{m}$  range, with a 2-pixel resolution of  $R \sim 2500$ . Immediately after V 773 Tau, we observed the nearby stars HD 27311 (A0) and HD 27560 (G0) to correct for telluric absorption features. The spectra were first sky-subtracted, corrected for distortion effects, flat-fielded and bad pixel-corrected.

To extract the individual spectra, we performed a fit to the binary profile along the spatial axis with a semi-empirical PSF. The latter is obtained by unfolding the Northern half of the profile of V 773 Tau AB, i.e., assuming a symmetric profile. The same profile was fitted to both components simultaneously. We estimate that the contamination of the spectrum of V 773 Tau D by that of V 773 Tau AB is less than 5% of the former at any wavelength. The continuum around  $\text{Br}\gamma$  in the spectra of V 773 Tau was not perfectly corrected with HD 27560, either because its spectrum is not close enough to the solar spectrum or because the telluric features changed between our observations. We thus divided both spectra by a third-order polynomial function fit to a 40 nm-wide window centered on  $\text{Br}\gamma$  and containing no other photospheric feature. The resulting spectrum of V 773 Tau AB in this window (except for about ten pixels around the hydrogen line itself) was used to correct the spectrum of V 773 Tau D of any remaining telluric feature. This procedure does not modify the shape

or strength of the Br $\gamma$  line in either spectrum but it improves significantly the continuum around that line. Finally, all spectra were divided by a fifth-order polynomial function fit to their respective continua. The output spectra are presented in Figure 3. The signal-to-noise ratio is estimated to be on the order of 100 per pixel in the final spectra.

### 3. Results

#### 3.1. A new stable quadruple system in Taurus

As can be seen in Figure 2, the system is clearly resolved in all our AO images into three components at a spatial resolution of  $0''.05$ – $0''.1$ . The brightest component at  $1.6$ – $3.8\,\mu\text{m}$  also dominates the flux in the visible and is associated with V 773 Tau AB, the SB discovered by Welty (1995). The latter cannot be resolved in our data; even at apoastron its projected separation on the sky is  $0''.0029$ . The three visual components are also simultaneously detected in the latest epochs of speckle imaging, from 1998 onward (see Figure 1). We attempted to re-analyze earlier datasets, but the fainter component did not show up because of the lower quality of earlier IR detectors, variability of the source and/or a less favorable configuration of the system. Our multiwavelength dataset unambiguously reveals that V 773 Tau AB has two distinct apparent companions.

By combining our new astrometric results with previous measurements, we can study the relative motion of these stars. We choose to use the rest frame of V 773 Tau AB. We exclude the 1991 measurement of Leinert et al. (1993) and the 1993  $J$  band measurement of Woitas et al. (2001) from our analysis. The former results are obtained from deprojecting the visibilities measured along two orthogonal axes while the latter are obtained with an instrument setup that does not provide Nyquist sampling of the PSF thus creating aliasing. Furthermore, to minimize the number of instrumental set-ups used in this analysis without reducing the time coverage of the orbit, we do not include the measurements presented in Tamazian et al. (2002). The locations of the companions as a function of time are illustrated in Figure 4. The motion of both visual companions to V 773 Tau AB are almost linear over the truncated 4 year time baseline 1998–2002, with velocities of  $18.0 \pm 0.4\,\text{mas/yr}$  at position angle  $125^\circ.1 \pm 2^\circ.1$  and  $13.7 \pm 1.1\,\text{mas/yr}$  along position angle  $120^\circ \pm 8^\circ$  for V 773 Tau C and V 773 Tau D respectively. While the proper motion of the system is of similar amplitude, its position angle is different ( $\sim 152^\circ$ , Frink et al. 1997), and it is unlikely that V 773 Tau D is a foreground/background object unrelated to the other components of V 773 Tau. This is further reinforced by the very small separation of the V 773 Tau AB–D pair. The surface density of  $K \leq 9.0$  objects (since  $K_{AB} \sim 7.0$ , Ghez, White & Simon 1997, we estimate that  $K_D \sim 9.0$ ) around V 773 Tau in the 2 Micron All-Sky Survey is about  $2.5 \times 10^{-6}$  per square

arcsecond. The probability of finding such a foreground/background object within  $0''.25$  of V 773 Tau AB is only  $\approx 5 \times 10^{-7}$ . We therefore conclude that V 773 Tau D really is physically associated with V 773 Tau, which is therefore a quadruple system.

With measurements regularly sampling the last twelve years, the orbit of V 773 Tau C is well defined. We therefore fit a Keplerian orbit to our astrometric dataset to constrain the orbital parameters, in particular the total system mass. We neglect here the influence of V 773 Tau D on the V 773 Tau AB–C system. We assumed that the orbit is closed ( $e < 1$ ), fixed the distance to  $D = 148$  pc, and explored the 7-dimension parameter space ( $P, a, e, i, \omega, \Omega, T_0$ ) using a  $\chi^2$  minimization routine. We used 10000 different starting points that were randomly selected within the allowed range for each orbital parameter to make sure that we converge on the absolute minimum of  $\chi^2$ . The resulting best fit orbit ( $\chi^2 = 1.94$ ) is shown in Figure 4 and the corresponding orbital parameters are presented in Table 2. The estimated inclination is very similar to the orbit of the SB (Welty 1995), suggesting a coplanar triple system. The derived periastron and apoastron distances are  $14 \pm 1$  AU and  $26 \pm 4$  AU respectively. Until relative radial velocities within the system are measured, an ambiguity on the inclination cannot be solved and, independently of this, the total system mass is only determined to within a distance-related scaling factor:  $M_{ABC} = (3.7 \pm 0.7) \times (D/148 \text{ pc})^3 M_\odot$ . Therefore, the uncertainty on the distance to the system (Lestrade et al. 1999) introduces an additional 10 % uncertainty on the system mass. Surprisingly, the uncertainties we estimate on the orbital parameters are not smaller than those derived by Tamazian et al. (2002) in spite of our extended coverage of the orbit. Some parameters differ by up to  $7\text{--}9\sigma$  ( $P_{orb}, a$ ) between the two orbital solutions, suggesting that Tamazian et al. underestimated their uncertainties.

The subsystem V 773 Tau ABC is a hierarchical triple system with a ratio of orbital periods of  $P_{AB-C}/P_{A-B} \gtrsim 300$ ; it is therefore expected to be dynamically stable over long timescales. On the other hand, the projected separation of V 773 Tau D is only slightly larger than the apoastron distance of V 773 Tau C, which raises the question of the stability of its orbit. Since V 773 Tau AB has such a compact orbit, we can consider it a single point mass. We apply the following criterion, derived by Eggleton & Kiseleva (1995) for a non-coplanar triple system to V 773 Tau AB–C–D: for a given combination of the mass ratios in a hierarchical system, there is a critical value of the ratio of the periastron distance of the outer pair to the apoastron separation of the inner binary beyond which the system can be considered stable for at least several hundred times the outer period. If this criterion is not fulfilled, there are times at which the three star-to-star distances in the system are commensurable, which is a highly unstable configuration. Applying this criterion with  $q_{in} = M_{AB}/M_C \approx 3.7$  and  $q_{out} = M_{ABC}/M_D \gtrsim 3.1$  (see § 4.1), we find that the orbit of V 773 Tau D is stable if its periastron distance is larger than about 115 AU. Since its projected separation



is about 30 AU, this suggests that its orbit is highly inclined to the line of sight ( $i \gtrsim 75^\circ$ , similar to the  $\sim 67^\circ$  inclination of both V 773 Tau AB and V 773 Tau C). If V 773 Tau D were on a circular orbit with such a radius, its predicted orbital velocity would be  $\sim 6$  km/s. This is very similar to its observed projected velocity with respect to the center of mass of V 773 Tau AB–C,  $V_D = 6.9 \pm 0.8$  km/s as measured from a linear fit to the motion of V 773 Tau D over the 1998–2002 period. Our astrometric dataset is therefore consistent with V 773 Tau D being on a stable, inclined orbit around the inner triple system.

### 3.2. SED and variability of the components of V 773 Tau

In an effort to understand the nature of V 773 Tau D, we first construct the SED of the system from 4000 Å up to 60  $\mu$ m. Unresolved photometry for the quadruple system is taken from White & Ghez (2001) in the visible, Rydgren & Vrba (1981) in the 1–4  $\mu$ m range and Prusti et al. (1992) for *IRAS* measurements<sup>5</sup>. Flux ratios within the system are from White & Ghez (2001) in the visible and from this study (our AO measurements) from 1.6  $\mu$ m to 3.8  $\mu$ m. No absolute photometric measurement of V 773 Tau is available at 4.7  $\mu$ m, so we did not use the results of our  $M'$  image in this analysis. Finally, we used the  $R$  band flux ratio of the SB from Welty (1995) to separate the contributions of V 773 Tau A and B. To correct for the foreground interstellar extinction, all measurements were dereddened with  $A_V = 1.39$  mag (Welty 1995, White & Ghez 2001) using a standard extinction law (Rieke & Lebofsky 1985). We assumed that none of the components of V 773 Tau was affected by circumstellar extinction. The resulting SED is presented in Figure 5.

We fit photospheric SEDs (as tabulated by Kenyon & Hartmann 1995) to the two components of the SB using the  $VRI$  photometry since this wavelength range is the least likely to be affected by accretion-induced excesses that can be present in TTS. Initially, the spectral types are considered to be those derived in the literature, K2 and K5 (Welty 1995), but a marginally better fit is obtained with spectral types K2 and K7 for V 773 Tau A and B respectively; the associated stellar luminosities are 2.2 and 1.4  $L_\odot$ , with an uncertainty of about 0.1  $L_\odot$ . White & Ghez (2001) obtained a similar value for the luminosity of V 773 Tau A although they estimated it based on the  $I$  band photometry only. We do not find evidence for any excess above photospheric levels up to 3.8  $\mu$ m for this pair. The unresolved spectrum of this pair displays many photospheric features, including a weak Br $\gamma$  absorption line (see

---

<sup>5</sup>The *IRAS* observations are blended with the CTTS FM Tau, which is located 40'' away. Prusti et al. (1992) were able to disentangle the contributions of both sources at 12 and 25  $\mu$ m. At 60  $\mu$ m, they assumed the same flux ratio as observed at 25  $\mu$ m. This extraction process results in large error bars (15 % and 20 % at 25 and 60  $\mu$ m respectively).

Figure 3). From a comparison of this spectrum with published spectra libraries (Kleinmann & Hall 1986; Wallace & Hinkle 1997), we estimate that the strength of the various features is compatible with a spectral type in the range K0–K5IV, consistent with the spectral types adopted here.

As already pointed out by White & Ghez (2001), the SED of V 773 Tau C can be fit with a pure photosphere from  $U$  to  $K$ . However, a  $\sim 3\sigma$  excess is then present at  $3.8\mu\text{m}$ , which is further reinforced by the fact that V 773 Tau C becomes brighter than V 773 Tau AB at  $M'$ . The nature of V 773 Tau C is revisited in § 4.1, where we argue that it is in fact a CTTS. For now, we only fit a photosphere to the visible measurements, and find a best fit for a spectral type M0.5 with a 1 subclass uncertainty and a  $1.5 \pm 0.2 L_{\odot}$  stellar luminosity, also in agreement with those obtained by White & Ghez (2001). This results in a  $\sim 0.2$  mag excesses at both  $H$  and  $K$ , a  $\sim 0.7$  mag excess at  $L'$  and a  $K - L' \approx 0.65 \pm 0.15$  mag color index. Broadly speaking, SED fitting is a trade-off between spectral type, luminosity and line-of-sight extinction. The assumption of identical extinction toward V 773 Tau C and V 773 Tau AB can be relaxed, in which case our estimated spectral type and luminosity are modified. With an additional 1 mag of extinction at  $V$  toward V 773 Tau C, we find that its SED is well fit by a K7 dwarf with a luminosity of  $2.3 \pm 0.3 L_{\odot}$ ; a significant excess at  $L'$  remains present although the  $H$  and  $K$  band fluxes are then consistent with photospheric levels. Larger extinctions are not allowed, since it would imply that more than  $0.8 L_{\odot}$  is absorbed by dust and reemitted at longer wavelengths, while this is the total observed mid-to far-infrared luminosity in the system (see below). We adopt here the “equal- $A_V$ ” estimates for V 773 Tau C, i.e. a M0.5 spectral type and a  $1.5 L_{\odot}$  luminosity.

In contrast to these three components, which can be fitted with normal photospheric colors and a moderate NIR excess for V 773 Tau C, V 773 Tau D displays extremely red colors ( $H - K \sim 1.3$  mag,  $K - L' \sim 1.7$  mag). A blackbody fit to its dereddened  $H, K, L'$  photometric data yields  $T_{NIR} = 900 \pm 200$  K, which is much cooler than any stellar photosphere. Its  $1.6\text{--}3.8\mu\text{m}$  SED is rising and this extends to longer wavelengths since V 773 Tau D is the brightest component of the system in our  $M'$  image, suggesting that it might be the dominant source of the unresolved mid-infrared flux of the system. Assuming that the *IRAS* fluxes can be fully assigned to V 773 Tau D, we conclude that the SED of this object presents a broad peak from  $\sim 5\mu\text{m}$  to  $\sim 30\mu\text{m}$  and that its bolometric luminosity is  $0.8 \pm 0.1 L_{\odot}$ . Since V 773 Tau C may exhibit a significant excess beyond the  $M'$  band, either through reprocessing of absorbed visible starlight or through emission of its disk, this value is an upper limit to the luminosity of V 773 Tau D. Nonetheless, we consider that the extremely red  $1.6\text{--}4.7\mu\text{m}$  colors of V 773 Tau D are substantial evidence that the mid-IR emission arises predominantly from this component. We also find that the spectrum of V 773 Tau D is remarkable in that it shows no photospheric features, in spite of the high signal-to-noise ratio of our data (Fig-

ure 3). The only significant feature in this spectrum is the  $\text{Br}\gamma$  line, which displays a weak emission with an equivalent width of  $0.4 \pm 0.1 \text{ \AA}$ . Since all photospheres have identifiable features in the observed wavelength range, we conclude that the NIR light we are receiving from V 773 Tau D has been thermally reprocessed by dust.

Finally, we note that at least some of the components in this system are photometrically variable, potentially increasing the uncertainties on the luminosities derived above. For instance, the flux ratio between V 773 Tau AB and V 773 Tau C varies by 1–1.5 mag both in the visible and the NIR (see Table 1). In fact, the resolved photometry presented by Ghez et al. (1997) suggests that V 773 Tau C is the variable component, as its  $K$  band magnitude varied by  $\sim 1$  mag while V 773 Tau AB remained almost unchanged. Furthermore, V 773 Tau AB, which dominates the flux of the system in the visible, has been shown to vary by only  $\sim 0.15$  mag in the visible (Rydgren & Vrba 1983). Similarly, the V 773 Tau AB to V 773 Tau D flux ratio at  $K$  band varied by  $\sim 1$  mag between 1998 and 2002 implying that V 773 Tau D is also variable. In the absence of simultaneous visible and NIR photometry for all components of the system, it is not possible to decide whether the variability of V 773 Tau C and V 773 Tau D is due to varying extinction along the line of sight or is intrinsic to these objects.

## 4. Discussion

### 4.1. Nature of the components of the system

#### 4.1.1. V 773 Tau AB and V 773 Tau C

V 773 Tau AB has so far been studied spectroscopically at optical wavelengths, under the assumption that the contamination by V 773 Tau C is negligible. The weakness of the  $\text{H}\alpha$  emission line in its spectrum (2–4  $\text{\AA}$  equivalent width; Herbig, Vrba & Rydgren 1986; Cabrit et al. 1990; Feigelson et al. 1994) as well as the chromospheric-like ultraviolet  $\text{Mg II } h$  and  $k$  emission lines (Feigelson et al. 1994), have led to a WTTS classification of both components of the SB. The observed  $\text{Br}\gamma$  line in absorption, the absence of NIR broadband excess in its SED up to  $L'$ , and the very limited amount of visible and NIR variability (§ 3.2) are also consistent with this classification, and we therefore adopt it. Based on their estimated spectral types and luminosities, White & Ghez (2001) concluded that  $M_A = 1.46 M_\odot$ . Our adopted luminosity is marginally larger, and we adopt  $M_A \approx 1.5 \pm 0.1 M_\odot$ . Using the dynamical mass ratio estimated by Welty (1995) for the SB, this implies a mass of  $\approx 1.1 M_\odot$  for V 773 Tau B.

The classification of V 773 Tau C as a WTTS by White & Ghez (2001) was based on its photopheric-like SED. However, as pointed out in § 3.2, it displays conclusive excesses at  $L'$  and  $M'$  as well as possible excesses at  $H$  and  $K$ . Its NIR excess is typical of CTTS and unheard of in WTTS. Similarly, the observed variability of V 773 Tau C in the visible and the NIR is typical of CTTS: variations of more than  $\sim 0.5$  mag in the visible and/or the NIR are generally associated with actively accreting TTS (Herbst et al. 1994; Skrutskie et al. 1996). It thus appears that V 773 Tau C is a CTTS, and such a classification resolves some of the puzzling properties of this system. These include the broad  $H\alpha$  emission line found by Feigelson et al. (1994), the strong  $\text{Br}\gamma$  emission line<sup>6</sup> measured by Folha & Emerson (2001) and the detection by Carbit et al. (1990) of visible forbidden emission lines, which are all atypical for a WTTS and rather suggest CTTS-like ongoing accretion and mass loss. All of these features can be explained if V 773 Tau C is a normal CTTS whose spectrum has been diluted by the spectrum of its bright WTTS neighbour since it accounts for only 20–30 % of the flux of the unresolved system. We therefore conclude that V 773 Tau C is a CTTS, which should be confirmed in the future by obtaining separate spectra for V 773 Tau AB and V 773 Tau C in the visible or the NIR.

Estimating the mass of V 773 Tau C is a non-trivial task, as it lies above the 1 Myr isochrone of the evolutionary model of Baraffe et al. (1998), with either M0.5 or K7 adopted as its spectral type, while V 773 Tau A falls on the 5 Myr isochrone (White & Ghez 2001). This is most likely because the luminosity of V 773 Tau C is partially contaminated by accretion-induced emission and is not purely photospheric. White & Ghez estimated an M0 spectral type and  $M_C = 0.7 M_\odot$  because the object lies in the HR diagram just above this almost vertical evolutionary track. Applying a similar reasoning, our K7–M0.5 estimated spectral type implies a stellar mass in the range 0.65–0.8  $M_\odot$ . We therefore adopt  $M_C = 0.7 \pm 0.1 M_\odot$ . The total mass of the V 773 Tau ABC triple system is therefore predicted to be  $3.3 \pm 0.2 M_\odot$ , which is in agreement with the dynamical mass we derived in § 3.1. While a finer analysis of the stellar masses in the system will require radial velocity measurements, this indicates that the stellar masses we adopt here are coherent with our dynamical analysis.

---

<sup>6</sup>In a  $1.3 \mu\text{m}$  spectrum obtained two nights earlier, they failed to detect the  $\text{Pa}\beta$  line in emission, even though it is usually stronger than the  $\text{Br}\gamma$  in CTTS (Muzerolle et al. 1998). This probably indicates that the emission lines are strongly variable.

#### 4.1.2. *V 773 Tau D is an “infrared companion”*

As noted in § 3.2, the SED of V 773 Tau D cannot be fit with any stellar photosphere and its spectrum suggests that this object is seen through optically thick dust. Therefore, it cannot be classified as a usual TTS. In fact, the shape of its SED matches that of a handful of objects first identified as IRCs to TTS by Chelli et al. (1988) and extensively studied by Koresko, Herbst & Leinert (1997). These companions were initially defined as extremely red, cool, objects located within a few hundred AU of a TTS. In agreement with our observations of V 773 Tau D, these IRCs have SEDs that are too broad to be fitted by single blackbody curves and that dominate the flux from the systems at wavelengths longer than 2–5  $\mu\text{m}$ . Furthermore,  $K$  band spectroscopy of several other IRCs have revealed featureless spectra, with the exception of Br $\gamma$  in emission (Beck, Prato & Simon 2001; Duchêne et al. 2002; Herbst, Koresko & Leinert 1995). Overall, we consider that the available dataset regarding V 773 Tau D clearly supports its classification as a new member of the small category of IRCs.

Although V 773 Tau D shares enough properties with other IRCs to be classified as such, it stands out from the other members of this class in at least two respects. The first remarkable property of V 773 Tau D is that its bolometric luminosity is not larger than that of the system’s primary. In fact, all other components in the system are intrinsically brighter than the IRC. The upper limit on its bolometric luminosity places a strict upper limit on its mass of about 1.2  $M_{\odot}$  (Baraffe et al. 1998, Palla & Stahler 1999, Siess et al. 2000), possibly significantly less if its luminosity is partially driven by accretion. Following the analysis of Do-Ar 24E by Koresko et al. (1997), we believe that the low luminosity of V 773 Tau D indicates that its mass is smaller than that of the other components in the system. We therefore conclude that  $M_D \lesssim 0.7 M_{\odot}$ .

The other noticeable property of V 773 Tau D can be found in the 8–13  $\mu\text{m}$  spectrum of the unresolved system presented by Hanner, Brooke & Tokunaga (1998), which displays no silicate feature, either in absorption or in emission. If the mid-infrared flux of V 773 Tau is dominated by the IRC, this contrasts with all other IRCs for which a spectrum has been obtained (Hanner et al. 1998; Natta, Meyer & Beckwith 2000) since they all present a strong, broad, spectral feature around 10  $\mu\text{m}$ . The absence of a silicate feature in the spectrum of V 773 Tau D is unlikely to be the result of a strong silicate depletion in its envelope, since this has not been observed among TTS. Possible explanations for this phenomenon include time variability of the feature, such as observed in the case of another IRC (Glass I, Gürtler et al. 1999), an accidental though almost exact cancellation of emission and absorption features in the envelope, the growth of most silicate grains beyond a few microns in size, or an unusually low temperature in the outer parts of the envelope. In cold environments ( $T \lesssim 100$  K), water ice can condense on and shield small silicates grains, in which case the grain opacity in the

mid-infrared does not show the usual marked features at  $10\,\mu\text{m}$  and  $20\,\mu\text{m}$  (e.g., Pollack et al. 1994). It is reasonable to expect that the outer parts of the dusty envelope surrounding V 773 Tau D are colder than that of other IRCs as it is a less luminous source, though the actual cause of the atypical mid-infrared spectrum of this source remains an open issue.

#### 4.1.3. *Nature of the IRCs*

The exact nature of IRCs is still debated. They may be normal TTS undergoing episodes of intense accretion and which are embedded in optically thick dusty envelopes with radii as small as a few AU (Ghez et al. 1991; Koresko et al. 1997; White & Ghez 2001; Duchêne et al. 2002). They also may be embedded protostars, i.e. objects in an earlier evolutionary phase (e.g., Ressler & Barsony 2001). This latter interpretation would imply that IRC binary systems are not coeval, in contradiction with results on large samples of TTS binaries (Hartigan, Strom & Strom 1994; White & Ghez 2001). We emphasize that the observational distinction between these two types of objects is quite limited; both are highly embedded sources whose flux is dominated by accretion onto and/or contraction of the central object (White & Ghez 2001), from which significant photometric variability can be expected. Photometric variability has indeed been documented for several IRCs (Ghez et al. 1991, Koresko et al. 1997), including V 773 Tau D (§ 3.2). Because IRCs are, by definition, encountered near few Myr-old T Tauri stars, it is difficult to imagine that they recently formed from the contraction of a vast (several thousand AU) envelope as normal T Tauri stars do, casting some doubt upon their protostellar nature. However, an isolated object with the same photometric and spectroscopic properties as V 773 Tau D would unambiguously be classified as an embedded protostar. The future detection of photospheric features in the spectrum of V 773 Tau D might clarify its properties, but for now we cannot conclusively determine the nature of this object.

Among the seven IRCs studied by Koresko et al. (1997), six were found to be more massive than their optically bright “primaries”, which suggested that their peculiarly dusty environment were a consequence of being the most massive component in the systems. However, the new IRC discovered here within V 773 Tau is found to be the lowest luminosity/mass object of the quadruple system. We therefore propose that there is a continuum of IRC masses and luminosities. In other words, there may be many yet undetected IRCs, as observational studies of such objects have likely been biased towards the brightest and therefore most massive ones. If so, we may expect that further deep, high-angular resolution  $10\text{--}20\,\mu\text{m}$  imaging around known TTS will reveal a significant population of much fainter objects with SEDs similar to that of V 773 Tau D.

#### 4.2. A “fully mixed” system

Most IRCs studied so far are associated with CTTS (Koresko et al. 1997). However, the quadruple system V 773 Tau consists of two  $1\text{--}1.5 M_{\odot}$  WTTS in a SB, a  $0.7 M_{\odot}$  CTTS orbiting around it at  $\sim 15\text{--}25$  AU, and a low-mass IRC located further away. This system can therefore be considered as a “fully mixed” system, containing all three types of TTS known so far: CTTS, WTTS and IRC. How it has evolved in the last Myr or so remains mysterious and it may even seem puzzling that a multiple system with two WTTS can also contain more active objects such as a CTTS and an IRC. However, one can speculate that strong interactions between the various components and their circumstellar environment have been major factors in its evolution.

The presence of two close companions located  $\sim 0.3$  AU and  $\sim 15$  AU away from V 773 Tau A can naturally explain why the two components of the SB have rapidly evolved toward WTTS. The various orbital motions would indeed clear out any circumstellar disk except in a narrow annulus between  $\sim 1\text{--}5$  AU (e.g., Artymowicz & Lubow 1994) within a few thousand years. Similarly, the circumstellar disk surrounding V 773 Tau C would be rapidly truncated to an outer radius of at most  $3\text{--}4$  AU. While the material surrounding V 773 Tau AB appears to have fully dissipated, V 773 Tau C still possesses an active accretion disk. However, the lifetime of such a small disk is relatively short unless it supports only a very small accretion rate. The upper limit on the millimeter thermal emission from the system corresponds to a maximum possible disk mass of only  $\sim 10^{-2} M_{\odot}$  (Beckwith et al. 1990; Dutrey et al. 1996). Given the age of the system and assuming that all this mass is located around V 773 Tau C, only a very low *time-averaged* accretion rate ( $\langle \dot{M} \rangle \lesssim 2 \times 10^{-9} M_{\odot}/\text{yr}$ ) could have allowed the disk to survive for so long. Most likely, this circumstellar disk is being replenished from an outer reservoir of material, as has already been suggested for tight pre-main sequence binaries (e.g., Prato & Simon 1997). The fact that V 773 Tau C seems to be the only component of the central triple system to be replenished may suggest that the orbital motion of the SB prevents material from falling deep into the potential well of V 773 Tau AB due to resonance interactions with the two stars.

Since it is on a much wider orbit, V 773 Tau D can retain a much larger envelope, several tens of AU in diameter, and its dissipation timescale may not be shorter than the age of the system. Although replenishment is not required to account for the presence of circumstellar material around this source, it is nonetheless surrounded by an unusually optically thick envelope. This may be a transient state generated through interactions with the other components of the system. In any case, V 773 Tau is the first system among T Tauri stars to display such a range of evolutionary states and it is likely that the compactness of the system, through strong star-star interactions, has an important role to play in this variety.

### 4.3. Do passive disks around TTS really exist?

The 5–60  $\mu\text{m}$  flux from V 773 Tau, that was previously assigned to a truncated, fossil, circumstellar/circumbinary disk around the WTTS system V 773 Tau AB, is now believed to be associated with the newly identified IRC, V 773 Tau D, with a possible contribution of the disk surrounding the CTTS V 773 Tau C. We conclude that there is no evidence for a fossil disk in this system.

Candidate fossil disks among pre-main sequence stars are quite rare. Skrutskie et al. (1990) and more recently Stassun et al. (2001) obtained 10  $\mu\text{m}$  photometry for relatively large samples (83 TTS and 32 WTTS respectively) and only identified a handful of such cases among pre-main sequence objects in Taurus and Orion. The most suggestive candidate is GM Aur which is known to be surrounded by a dusty disk in Keplerian rotation (Koerner, Sargent & Beckwith 1993) but shows at best a marginal photometric excess shortwards of 10  $\mu\text{m}$  (Stassun et al. 2001, White & Ghez 2001). However, this object presents a strong accretion-induced ultraviolet/blue excess and it is unclear whether it should be classified as a passive disk. About ten other objects, or roughly 10 % of the combined sample, might fall in this category, suggesting a lifetime for this phenomenon on order of a few  $10^5$  yrs.

However, our analysis of V 773 Tau has led us to remove this system from the list of candidate fossil disks and one may wonder whether other systems will similarly be reclassified out of this category by further analysis. If so, fossil disks would be extremely short-lived structures. As we have shown here, the presence of a close, unresolved IRC in the vicinity of a WTTS can be misinterpreted as a passive disk on the basis of its SED. Similarly, a tight SB would rapidly clear a central gap in its surrounding disk and the absence of the hottest parts of the disk would result in a dip in the NIR part of the SED of the system (e.g., Mathieu et al. 1991). A disk inner radius of about 0.4 AU results in no excess above photospheric levels up to 5  $\mu\text{m}$  or so, similar to the SED of a passive disk. Such an inner radius can be created by a binary with a semi-major axis of about 0.15 AU (Artymowicz & Lubow 1994), corresponding to an orbital period of about 20  $d$  for a  $1 M_\odot$  total system mass. Unresolved IRCs and short period SBs can therefore mimic passive disks, and it is therefore important to compare the frequencies of these various systems to decide whether a significant proportion of passive disks really exists among pre-main sequence stars.

So far, at least five IRCs out of  $\sim 100$  pre-main sequence objects are known in Taurus (T Tau Sa, Haro 6-10 N, XZ Tau B, UY Aur B and now V 773 Tau D) and more may be discovered when 5–10  $\mu\text{m}$  high-angular images of large samples of TTS are performed. This



observed proportion of  $\sim 5\%$  of IRCs is therefore only a lower limit<sup>7</sup>. The proportion of SBs with  $P_{orb} < 20 d$  for solar-type main sequence objects is estimated to be about 4–5% (Duquennoy & Mayor 1991), and it might be even higher among young stars in Taurus as is the case for visual binaries (e.g., Ghez et al. 1993). To the best of our knowledge, only 4 such short-period SBs are known among the Taurus pre-main sequence population, out of which only 2 (V 826 Tau, Mundt et al. 1983, and LkCa 3, Mathieu 1994) are classified as WTTS based on their visible/NIR photometric and spectral properties. Overall, the proportion of passive disks ( $\lesssim 10\%$ ) qualitatively matches those of IRCs and short period SBs among pre-main sequence stars (both  $\gtrsim 5\%$ ). It is very possible that most (if not all) fossil disks candidates are in fact associated with currently unknown IRCs or SBs. More generally, this emphasizes how dangerous SED analyses are if all stellar components have not been resolved. This issue, which was suggested by Chelli et al. (1988) and Ghez (1996), resurfaces as a concern with the advent of IR missions with only moderate spatial resolution ( $\gtrsim 1''$ ), such as SIRTf and SOFIA.

## 5. Conclusion

Using speckle interferometry techniques at the 10m Keck I and 200-inch Hale telescopes and the AO system on Keck II, we have obtained multi-epoch high-angular resolution images of the multiple system V 773 Tau in the visible and the NIR throughout the last decade. It had been considered one of the rare examples of the so-called “passive” or “fossil” disks which are thought of as disks in which planetesimals have formed in the inner parts, thus halting the accretion process on the stars without expelling the outer disk material.

In addition to the unresolved SB V 773 Tau AB and the previously known speckle companion V 773 Tau C, we identify a  $K \sim 9$ ,  $K - L' \sim 1.7$  mag, fourth component in our AO images and in some speckle datasets. V 773 Tau D, which is located only  $0''.2$  away from V 773 Tau AB, is the brightest source in the system at  $4.8 \mu\text{m}$ . We have also obtained medium-resolution  $2 \mu\text{m}$  spectra of V 773 Tau AB and V 773 Tau D. Given its NIR brightness, its location, and its apparent motion, we conclude that the newly identified component is physically associated with the system. We fit the motion of V 773 Tau C around V 773 Tau AB with a closed Keplerian orbit, and we conclude that the quadruple system can be dynamically stable provided V 773 Tau D is on a highly inclined orbit, as are the other orbits within

---

<sup>7</sup>IRCs constitute a significant fraction of the “high accretion rate” population identified by White & Ghez (2001) in Taurus on the basis of the extremely red colors of these objects ( $K - L > 1.4$ , as is the case for V 773 Tau D). Roughly 10% of all TTS belong to this other category, in qualitative agreement with our estimated proportion of IRCs.

the system. As opposed to T Tau (Loinard et al. 2003), this system does not support the proposed explanation to the observed overabundance of young high-order multiple systems that many of them are in fact unstable systems that will rapidly decay into an ejected single star and a lower order multiple system (Ghez et al. 1993; Reipurth 2000).

Analysis of the SED of the system and of our spectra supports the following picture: both components of V 773 Tau AB are  $1\text{--}1.5 M_{\odot}$  WTTS, V 773 Tau C is a lower-mass variable CTTS and V 773 Tau D is a new member of the IRC category, i.e. a deeply embedded companion to a normal T Tauri star. The properties of this new object include a broadly peaked SED from  $\sim 5\text{--}20 \mu\text{m}$ , significant variability at  $2 \mu\text{m}$ , and a featureless  $2 \mu\text{m}$  spectrum. Its low bolometric luminosity ( $L_D \lesssim 0.8 L_{\odot}$ ) shows that it is the least massive component of the system, in contrast to most other IRCs. We suggest that many low-mass IRCs might remain to be discovered. The physical nature of IRCs remains unconstrained since both embedded T Tauri stars or less evolved protostars are almost identical in terms of their observable properties.

The immediate implication of the presence of V 773 Tau D is the rejection of the hypothesis of a passive disk in the system since the long known IR excess is now attributed to the IRC. Given the estimated proportions of IRCs and short period SBs, we argue that the frequency of passive disks among pre-main sequence stars may have been strongly overestimated in the past and that the lifetime of this transition phase may be much shorter than previously thought. More generally, our analysis of V 773 Tau shows how cautious one must be when using NIR or mid-IR photometry of TTS obtained with low spatial resolution devices.

Part of the data presented herein were obtained at the W. M. Keck Observatory, which is operated as a scientific partnership among the California Institute of Technology, The University of California, and the National Aeronautics and Space Administration. The Observatory was made possible by the generous financial support of the W. M. Keck Foundation. We gratefully thank the staff at Palomar and Keck observatories for their assistance during the observations as well as Bruce Macintosh for his help during the acquisition of part of the data presented in this study. A detailed report by an anonymous referee significantly helped improve this manuscript. Frank Marchis kindly provided the synthetic PSFs that were used in this study.

This work has been supported in part by the National Science Foundation Science and Technology Center for Adaptive Optics, managed by the University of California at Santa Cruz under cooperative agreement AST 98-76783, by NASA’s Origins of Solar System program grant NAG-6975, and by the Packard Foundation. This research has made use of

the SIMBAD database, operated at CDS, Strasbourg, France. The authors wish to recognize and acknowledge the very significant cultural role and reverence that the summit of Mauna Kea has always had within the indigenous Hawaiian community. We are most fortunate to have the opportunity to conduct observations from this mountain.

## REFERENCES

- Anosova, Z. P. 1986, *Ap&SS*, 124, 217
- Artymowicz, P. & Lubow, S. H. 1994, *ApJ*, 421, 651
- Baraffe, I., Chabrier, G., Allard, F. & Hauschildt, P. H. 1998, *A&A*, 337, 403
- Beck, T. L., Prato, L. & Simon, M. 2001, *ApJ*, 551, 1031
- Beckwith, S. V. W., Sargent, A. I., Chini, R. S. & Guesten, R. 1990, *AJ*, 99, 924
- Cabrit, S., Edwards, S., Strom, S. E. & Strom, K. M. 1990, *ApJ*, 354, 687
- Chelli, A., Cruz-Gonzalez, I., Zinnecker, H., Carrasco, L. & Perrier, C. 1988, *A&A*, 207, 46
- Duchêne, G., Ghez, A. M. & McCabe, C. 2002, *ApJ*, 568, 771
- Duquennoy, A. & Mayor, M. 1991, *A&A*, 248, 485
- Dutrey, A., Guilloteau, S., Duvert, G., Prato, L., Simon, M., Schuster, K. & Ménard, F. 1996, *A&A*, 309, 493
- Eggleton, P. & Kisseleva, L. 1995, *ApJ*, 455, 640
- Feigelson, E. D. & Kriss, G. A. 1989, *ApJ*, 338, 262
- Feigelson, E. D., Welty, A. D., Imhoff, C. L., Hall, J. C., Etzel, P. B., Phillips, R. B. & Lonsdale, C. J. 1994, *ApJ*, 432, 373
- Folha, D. F. M. & Emerson, J. P. 2001, *A&A*, 365, 90
- Frink, S., Röser, S., Neuhäuser, R. & Sterzik, M. F. 1997, 325, 613
- Ghez, A. M., Neugebauer, G. & Matthews, K. 1993, *AJ*, 106, 2005
- Ghez, A. M., Weinberger, A. J., Neugebauer, G., Matthews, K. & McCarthy, D. W. Jr. 1995, *AJ*, 110, 753

- Ghez, A. M. 1996, in “Evolutionary Processes in Binary Stars”, R. A. M. J. Wijers, M. B. Davies and C. A. Tout eds., Kluwer Academic Publishers, NATO ASI Series C, Mathematical and Physical Sciences, 477, 1
- Ghez, A. M., White, R. J. & Simon, M. 1997, *ApJ*, 490, 353
- Gorham, P. W., Ghez, A. M., Hannif, C. A., Kulkarni, S. R., Matthews, K. & Neugebauer, G. 1992, *AJ*, 103, 953
- Gürtler, J., Schreyer, K., Henning, T., Lemke, D. & Pfau, W. 1999, *A&A*, 346, 205
- Hanner, M. S., Brooke, T. Y. & Tokunaga, A. T. 1998, *ApJ*, 502, 871
- Hartigan, P., Strom, K. M. & Strom, S. E. 1994, *ApJ*, 427, 961
- Herbig, G. H. & Rao Kameswara, N. 1972, *ApJ*, 174, 401
- Herbig, G. H. 1977, *ApJ*, 214, 747
- Herbig, G. H., Vrba, F. J. & Rydgren, A. E. 1986, *AJ*, 91, 57
- Herbst, W., Herbst, D. K., Grossman, E. J. & Weinstein, D. 1994, *AJ*, 108, 1906
- Herbst, T. M., Koresko, C. D. & Leinert, C. 1995, *ApJ*, 444, L93
- Kenyon, S. J. & Hartmann, L. 1995, *ApJS*, 101, 117
- Kleinmann, S. G. & Hall, D. N. B. 1986, *ApJS*, 62, 501
- Koerner, D. W., Sargent, A. I. & Beckwith, S. V. W. 1993, *Icarus*, 106, 2
- Koresko, C. D., Herbst, T., M. & Leinert, C. 1997, *ApJ*, 480, 741
- Leinert, C., Zinnecker, H., Weitzel, N., Christou, J., Ridgway, S. T., Jameson, R., Haas, M. & Lenzen, R. 1993, *A&A*, 278, 129
- Lestrade, J.-F., Preston, R. A., Jones, D. L., Phillips, R. B., Rogers, A. E. E., Titus, M. A., Rioja, M. J. & Gabudza, D. C. 1999, *A&A*, 344, 1014
- Loinard, L., Rodríguez, L. F. & Rodríguez, M. I. 2003, *ApJL*, in press
- Massi, M., Menten, K. & Neidhöfer, J. 2001, *A&A*, 382, 152
- Mathieu, R. D., Fred, A. C. & Latham, D. W. 1991, *AJ*, 101, 2184
- Mathieu, R. D. 1994, *ARA&A*, 32, 465

- Matthews, K. & Soifer, B. T. 1994, *ExA*, 3, 77
- Matthews, K., Ghez, A. M., Weinberger, A. J. & Neugebauer, G. 1996, *PASP*, 108, 615
- McLean, I. S., Graham, J. R., Becklin, E. E., Figer, D. F., Larkin, J. E., Levenson, N. A. & Teplitz, H. I. 2000, *SPIE*, 4008, 1048
- Mundt, R., Walter, F. M., Feigelson, E. D., Finkenzeller, U., Herbig, G. H. & Odell, A. P. 1983, *ApJ*, 269, 229
- Muzerolle, J., Hartmann, L. & Calvet, N. 1998, *AJ*, 116, 2965
- Natta, A., Meyer, M. R. & Beckwith, S. V. W. 2000, *ApJ*, 534, 838
- O’Neal, D., Feigelson, E. E., Mathieu, R. D. & Myers, P. C. 1990, *AJ*, 100, 1610
- Palla, F. & Stahler, S. W. 1999, *ApJ*, 525, 772
- Patience, J., Ghez, A. M., Reid, I. N., Weinberger, A. J. & Matthews, K. 1998, *AJ*, 115, 1972
- Phillips, R. B., Lonsdale, C. J., Feigelson, E. D. & Deeney, B. D. 1996, *AJ*, 111, 918
- Pollack, J. B., Hollenbach, D., Beckwith, S. V. W., Simonelli, D. P., Roush, T. & Fong, W. 1994, *ApJ*, 421, 615
- Prato, L. & Simon, M. 1997, *ApJ*, 474, 455
- Prusti, T., Clark, F. O., Laureijs, R. J., Wakker, B. P. & Wesselius, P. R. 1992, *A&A*, 259, 537
- Reipurth, B. 2000, *AJ*, 120, 3177
- Ressler, M. E. & Barsony, M. 2001, *AJ*, 121, 1098
- Rieke, G. H. & Lebofsky, M. J. 1985, *ApJ*, 288, 618
- Rydgren, A. E. & Vrba, F. J. 1981, *AJ*, 86, 1069
- Rydgren, A. E. & Vrba, F. J. 1983, *ApJ*, 267, 191
- Siess, L., Dufour, E. & Forestini, M. 2000, *A&A*, 358, 593
- Skrutskie, M. F., Dutkevitch, D., Strom, S. E., Edwards, S. & Strom, K. M. 1990, *AJ*, 99, 1187

- Skrutskie, M. F., Meyer, M. R., Whalen, D. & Hamilton, C. 1996, *AJ*, 112, 2168
- Stassun, K. G., Mathieu, R. D., Vrba, F. J., Mazeh, T. & Henden, A. 2001, *AJ*, 121, 1003
- Strom, S. E. 1995, *RMxAC*, 1, 317
- Wallace, L. & Hinkle, K. 1997, *ApJS*, 111, 445
- Welty, A. D. 1995, *AJ*, 110, 776
- White, R. J. & Ghez, A. M. 2001, *ApJ*, 556, 265
- Wizinowich, P., Acton, D. S., Shelton, C., Stomski, P., Gathright, J., Ho, K., Lupton, W., Tsubota, K., Lai, O., Max, C., Brase, J., An, J., Avicola, K., Olivier, S., Gavel, D., Macintosh, B., Ghez, A. M., Larkin, J. E. 2000, *PASP*, 112, 315
- Woitas, J., Köhler, R. & Leinert, C. 2001, *A&A*, 369, 249

Table 1. Summary of all spatially resolved measurements of the V 773 Tau system.

Date	Obs. Tech.	Filter	V 773 Tau AB–C			V 773 Tau AB–D			Ref.
			$\rho$ (mas)	$\theta$ (°)	$\Delta m$ (mag)	$\rho$ (mas)	$\theta$ (°)	$\Delta m$ (mag)	
1990 Oct 03	Spk	<i>K</i>	112±2	295±4	0.80±0.03	(...)	(...)	(...)	2
1991 Sep 21	1D <sup>a</sup>	<i>K</i>	170±10	295±3	2.22±0.33	(...)	(...)	(...)	3
1991 Sep 25–29	Spk	<i>F</i> <sub>620</sub>	106±5	298±2	2.94±0.10	(...)	(...)	(...)	1
”	”	<i>F</i> <sub>656</sub>	”	”	2.19±0.10	(...)	(...)	(...)	1
”	”	<i>F</i> <sub>800</sub>	”	”	2.05±0.10	(...)	(...)	(...)	1
”	”	<i>F</i> <sub>850</sub>	”	”	2.19±0.10	(...)	(...)	(...)	1
1992 Oct 10	Spk	<i>K</i>	120±20	307±5	1.71±0.01	(...)	(...)	(...)	4,5
1993 Oct 05	Spk <sup>b</sup>	<i>J</i>	111±4	308.9±1.4	2.37±0.05	(...)	(...)	(...)	6
1993 Nov 25	Spk	<i>K</i>	92±8	304±8	1.75±0.22	(...)	(...)	(...)	4,5
1994 Oct 19	Spk	<i>K</i>	65.6±1.4	318±2	0.46±0.04	(...)	(...)	(...)	4,5
1994 Oct 29	<i>HST</i>	<i>U'</i>	62.8±2.4	321.9±2.7	1.89±0.78	(...)	(...)	(...)	5
”	”	<i>B'</i>	”	”	2.78±0.92	(...)	(...)	(...)	5
”	”	<i>V'</i>	”	”	1.73±0.44	(...)	(...)	(...)	5
”	”	<i>R'</i>	”	”	1.36±0.37	(...)	(...)	(...)	5
”	”	<i>I'</i>	”	”	1.19±0.54	(...)	(...)	(...)	5
1996 Oct 24	Spk <sup>c</sup>	<i>K</i>	(...)	(...)	(...)	162±29	176±5	2.17±0.27	1
1997 Nov 19	Spk <sup>c</sup>	<i>K</i>	(...)	(...)	(...)	187.7±3.9	173.7±1.5	2.12±0.10	1
1998 Nov 04	Spk	<i>K</i>	57.4±1.2	67.1±1.4	0.76±0.03	191.3±3.6	164.7±1.3	2.85±0.06	1
1999 Nov 20	Spk	<i>K</i>	74.4±1.4	81.9±1.1	0.83±0.06	202.4±3.8	161.3±2.0	2.79±0.05	1
2000 Nov 20	AO	<i>H</i>	85±3	88.4±1.5	0.44±0.10	212±4	155.7±0.7	2.86±0.15	1
”	”	<i>K</i>	”	”	0.46±0.05	”	”	1.92±0.10	1
2000 Dec 08	Spk	<i>K</i>	91.1±3.9	88.5±1.2	1.01±0.07	217.4±4.9	159.3±4.9	2.43±0.07	1
2001 Feb 08	Spk <sup>d</sup>	<i>K</i>	95±5	93.5±0.6	(...)	(...)	(...)	(...)	7
2001 Nov 02	Spk <sup>d</sup>	<i>K</i>	99±7	94.6±1.0	(...)	(...)	(...)	(...)	7
2001 Dec 08	Spk	<i>K</i>	100.0±1.0	92.3±1.0	0.33±0.07	223.0±3.0	154.1±1.0	1.84±0.07	1
2002 Dec 13	AO	<i>L'</i>	116.5±2.0	100.6±0.7	0.06±0.05	237±3	153.7±0.6	0.36±0.05	1
”	”	<i>M'</i>	”	”	-0.21±0.05	”	”	-0.30±0.05	1

Note. — The data presented in this table have been obtained through two-dimensional (“Spk”) and one-dimensional (“1D”) speckle interferometry, AO or *HST*/WFPC2 imaging.  $\rho$  represents the binary separation and  $\theta$  its position angle as measured East from North on the sky. In all observations between 1990 and 1997, only one companion was unambiguously detected.

<sup>a</sup>This measurement was obtained by analyzing two orthogonal one-dimension scans and retrieving the actual separation and position angle by deprojection from these axes. The uncertainties associated with this method are significantly larger from those associated with two-dimension speckle measurements, and this data point differs by more than  $5\sigma$  from the visible 2D speckle result we obtained just a week later, suggesting that the uncertainties of the 1D measurement are underestimated. It has not been included in our final analysis.

<sup>b</sup>Instead of being a Nyquist-sampled measurement, this dataset was obtained with a pixel scale that is almost equal to the diffraction limit of the 3.5 m Calar Alto telescope in the *J* band (0''.07/pixel and 0''.074 respectively). This measurement is thus significantly aliased and therefore has not been used in our analysis.

<sup>c</sup>In these measurements, the tight pair V 773 Tau AB–C was not fully resolved. All photometric and astrometric information extracted from this dataset therefore pertains to the V 773 Tau ABC–D system.

<sup>d</sup>These measurements were obtained with a different instrumental and calibration set-up than most of our data. To minimize the effect of systematic differences between datasets, we do not include these datasets in our analysis since our own data already provide an adequate time sampling throughout the 1998–2002 period.

References. — 1) This work; 2) Ghez et al. (1993); 3) Leinert et al. (1993); 4) Ghez et al. (1995); 5) Ghez et al. (1997); 6) Woitas et al. (2001); 7) Tamazian et al. (2002).

Table 2. Parameters for the orbit of V 773 Tau C around V 773 Tau AB.

$M_{ABC}(M_{\odot})$	$P_{orb}$ (yrs)	$a$ (AU)	$e$	$i$ ( $^{\circ}$ )	$T_0$	$\omega$ ( $^{\circ}$ )	$\Omega$ ( $^{\circ}$ )
$3.7 \pm 0.7^a$	$46 \pm 6$	$20 \pm 1$	$0.3 \pm 0.1$	$66 \pm 3^b$	$1996.5 \pm 0.8$	$81 \pm 10^b$	$288 \pm 1^b$

<sup>a</sup>The uncertainty on the total system mass only includes the fitting uncertainty. An additional 10 % random uncertainty arises from the error on the distance to the system since orbital analysis relying on astrometric data only constrains  $M_{syst}/D^3$ .

<sup>b</sup>In the absence of radial velocity measurements, an ambiguity in the inclination angle remains unsolvable. We have *assumed* that  $i < 90^{\circ}$ , which means that V 773 Tau C is currently in front of the other component. However, it is equally possible that  $i = 114^{\circ}$ , in which case  $\omega = 279^{\circ}$  and  $\Omega = 108^{\circ}$ . The uncertainties on these parameters, as well as the location of periastron, are however unaffected by this ambiguity.



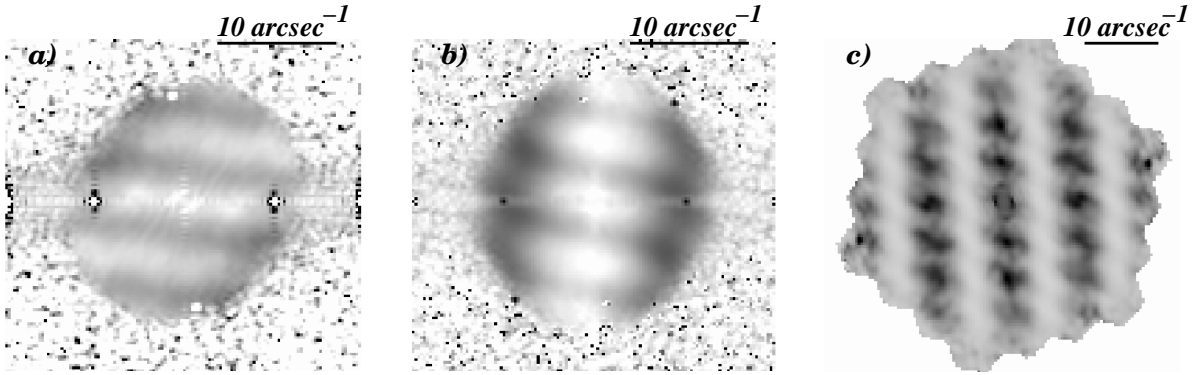


Fig. 1.— Examples of speckle interferometry power spectra of the V 773 Tau system obtained in 1997 (*a*), 1999 (*b*) and 2001 (*c*). In the first epoch, only the V 773 Tau AB–D pair, oriented more or less North-South is clearly detected. In the later two epochs, a set of much wider fringes appears, corresponding to a tight pair oriented roughly East-West, V 773 Tau AB–C. In the 2001 dataset, it is particularly clear that two independent sets of fringes are detected or, equivalently, that the system is resolved into three different components. Note the different spatial scales for the Palomar (*a* and *b*) and Keck (*c*) datasets, which explains why the fringes associated to the V 773 Tau AB–C pair in the latter show several cycles in the Fourier space instead of merely one.

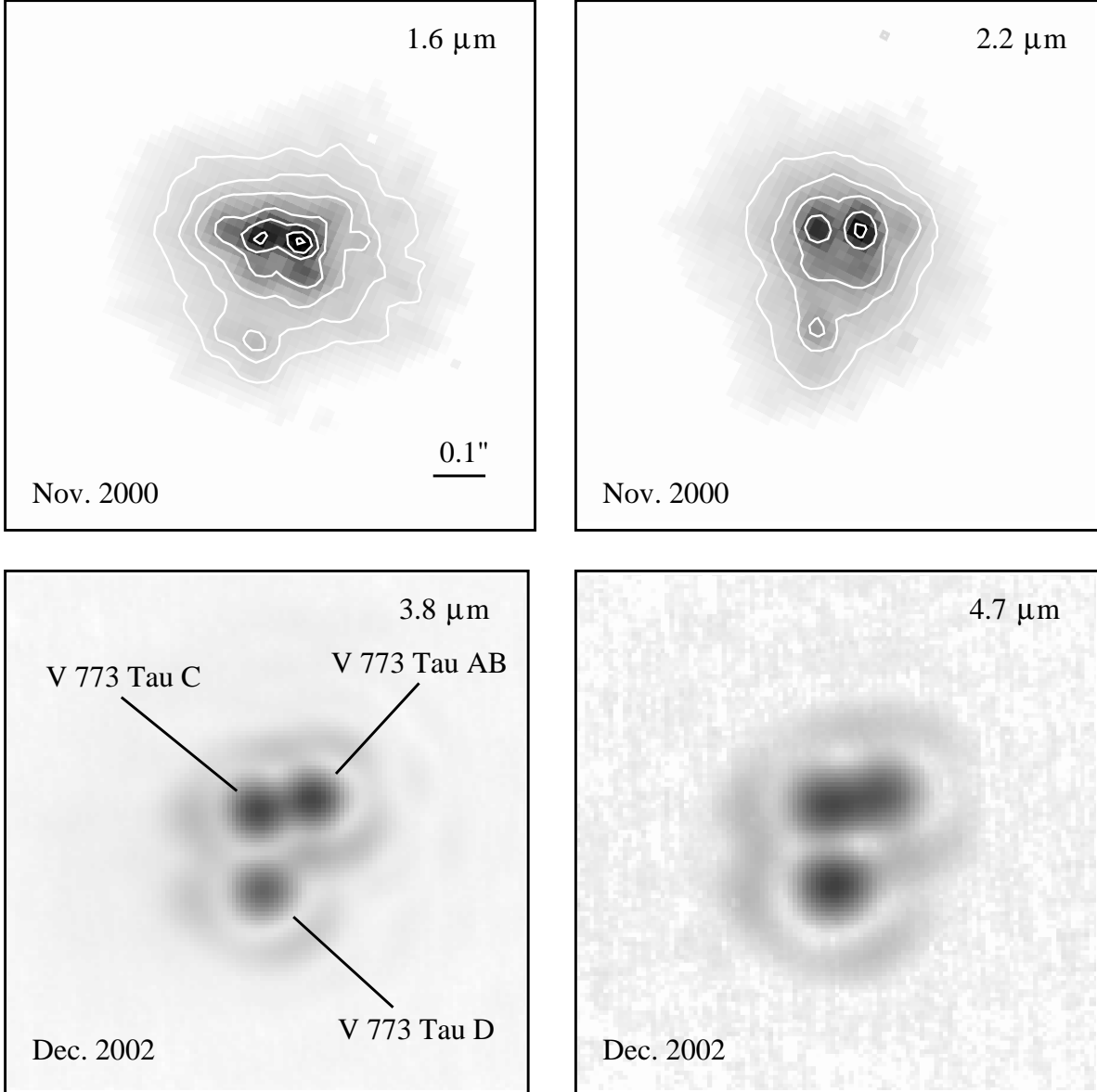


Fig. 2.— Adaptive optics images of the V 773 Tau multiple system obtained in November 2000 (top row) and December 2002 (bottom row). A square root stretch has been used in all images. North is up and East to the left and each image is 1'' across. The lowest contour in the  $H$  and  $K$  images is about 120 times and 150 times higher than the background noise. The contours represent 2 %, 3 %, 5 %, 15 %, 33 %, 60 % and 90 % of the peak value in the  $H$  band image and 3 %, 7 %, 15 %, 45 % and 90 % of the peak at  $K$ . The motion of V 773 Tau C with respect to V 773 Tau AB between the two epochs is particularly obvious in these images, as well as the relative brightening of V 773 Tau D towards longer wavelengths.

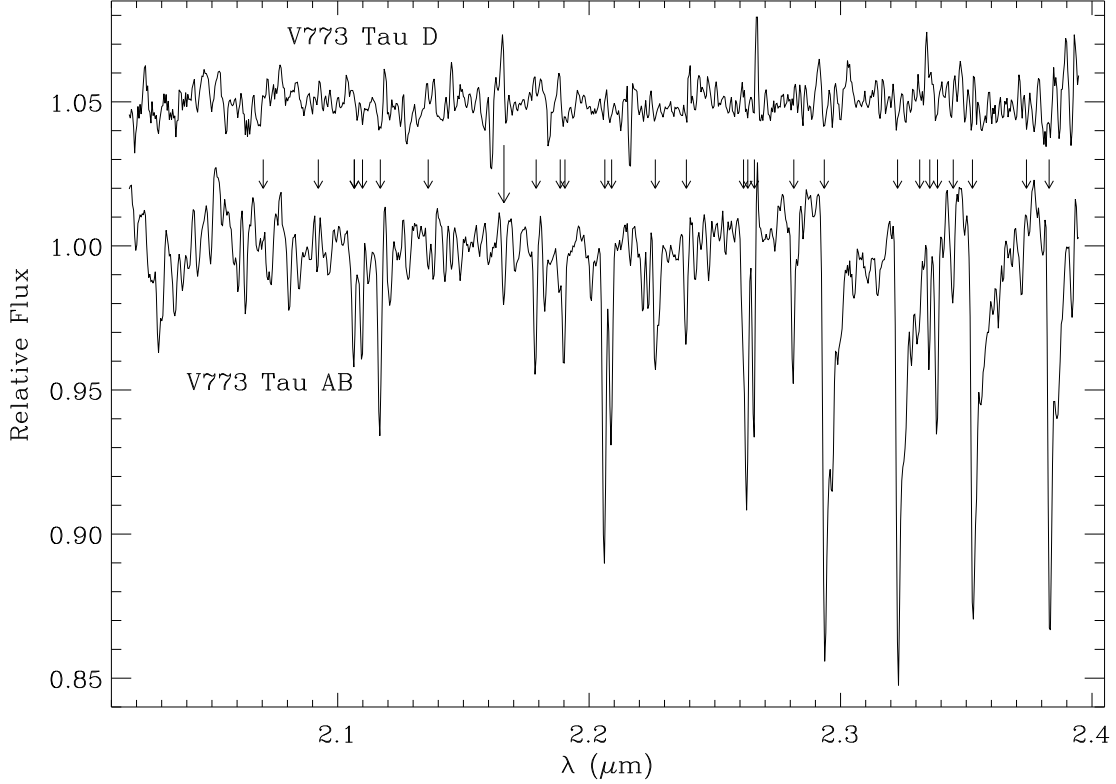


Fig. 3.— Continuum-normalized spectra of V 773 Tau AB and V 773 Tau D; the latter has been shifted upwards by 0.05 for clarity. The arrows indicate all known spectral features in this wavelength range (Kleinmann & Hall 1986) and the Br $\gamma$  line is indicated by the longer arrow. Both spectra have been smoothed down to a resolution of about  $R \sim 1900$ . A few spikes, both in emission and in absorption, appear in the spectrum of V 773 Tau D but they are too narrow (typically 1 pixel-wide) to be real features. Furthermore, similar “features” can be seen in the spectrum of V 773 Tau AB (e.g., at 2.217  $\mu\text{m}$  or 2.267  $\mu\text{m}$ ), which suggests that they correspond to poorly corrected telluric absorption lines.

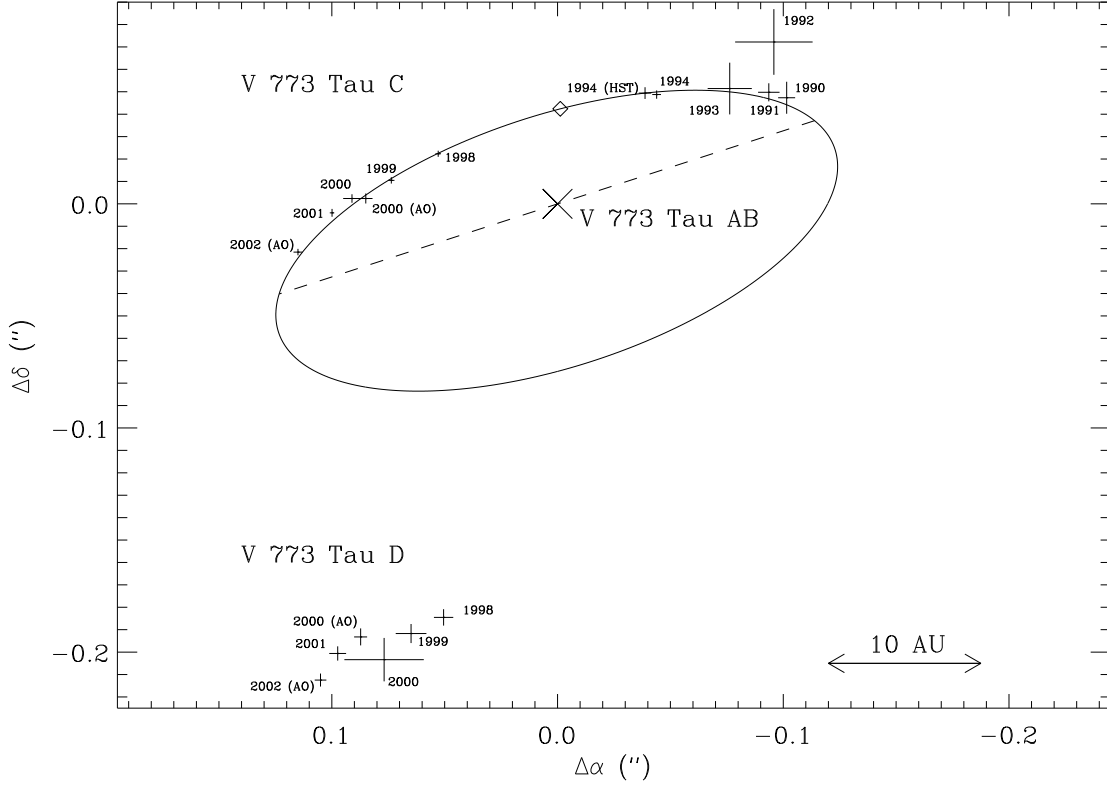


Fig. 4.— Location of the companions that have been spatially resolved from V 773 Tau AB since 1990. The SB (large cross) is fixed at location (0,0); the amplitude of the internal orbital motion of V 773 Tau AB is negligible at the scale of this figure. The length of the tick marks indicate  $1\sigma$  error bars and the year of observation is associated to each point. Only the datapoints used in the dynamical analysis are shown here. Our best fit orbit for V 773 Tau C is represented by the solid curve, together with its periastron (open diamond) and line of nodes (dashed line).

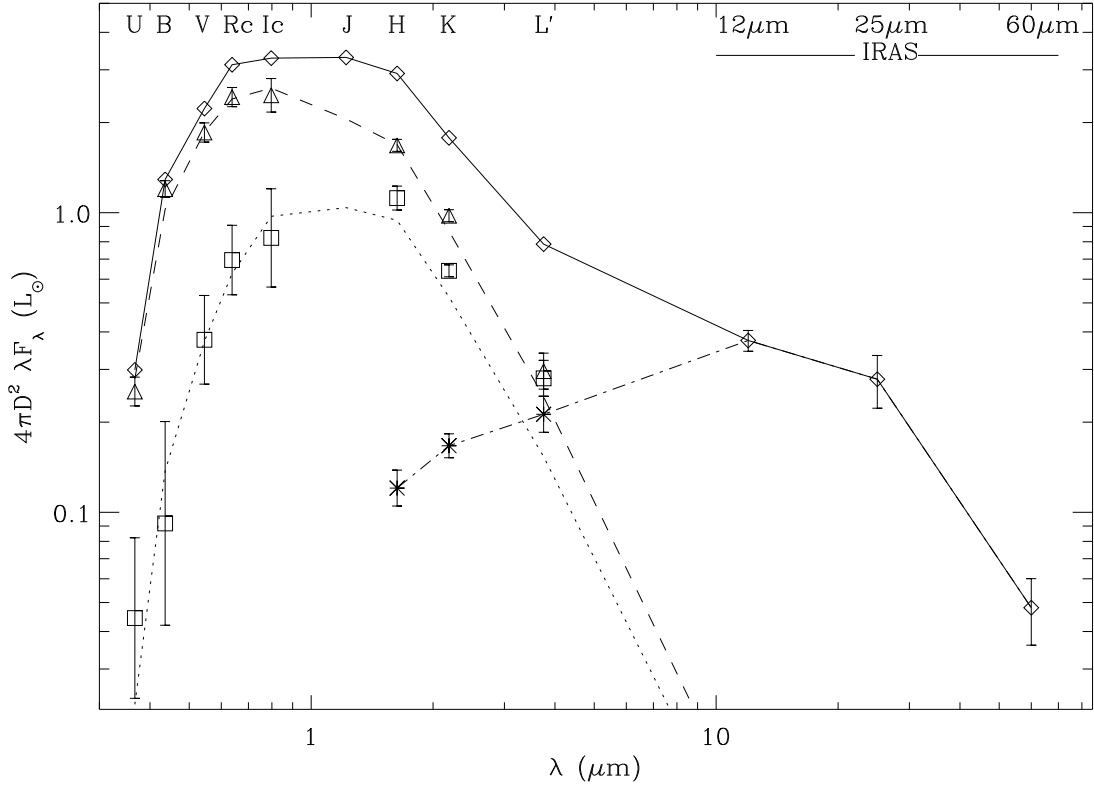


Fig. 5.— Dereddened SED of the components of the system. *Diamonds*: unresolved system; *triangles*: V 773 Tau AB; *squares*: V 773 Tau C; *asterisks*: V 773 Tau D. The dashed curve is the sum of the K2 and K7 photospheres fitted to the components of V 773 Tau AB while the dotted curve is the M0.5 photosphere fit to V 773 Tau C. The dot-dashed curves joins the observed *HKL'* photometric points for V 773 Tau D with the unresolved *IRAS* measurements.